

Signatures of dynamical processes in Raman lidar profiles of the atmosphere

C. Russell Philbrick^{*1,2} and Hans D. Hallen¹

¹Physics Department and ²Marine, Earth, and Atmospheric Sciences Department
N. C. State University, Raleigh NC, 27692-8202

ABSTRACT

Raman lidar measurements provide profiles of several different tracers of spatial and temporal variations, which are excellent signatures for studies of dynamical processes in the atmosphere. An examination of Raman lidar data collected during the last four decades clearly show signatures of atmospheric planetary waves, gravity waves, low-level jets, weather fronts, turbulence from wind shear at surfaces and at the interface of the boundary layer with the free troposphere. Water vapor profiles are found to be important as a tracer of the sources of turbulence eddies associated with thermal convection, pressure waves, and wind shears, which result from surface heating, winds, weather systems, orographic forcing, and regions of reduced atmospheric stability. Examples of these processes are selected to show the influence of turbulence on profiles of atmospheric properties. Turbulence eddies generated in the wind shear region near the top of the boundary layer are found to mix into the atmospheric boundary layer. Results from several prior research projects are examined to gain a better understanding of processes impacting optical propagation through the many sources of turbulence observed in the lower atmosphere. Advances in lasers, detectors, and particularly in high-speed electronics now available are expected to provide important opportunities to improve our understanding of the formation processes, as well as for tracking of the sources and dissipation of turbulence eddies.

Keyword list: Raman lidar, troposphere dynamics, turbulence eddies, thermal convection, wind shear turbulence, atmospheric boundary layer, marine boundary layer, water vapor profiles, signatures of dynamics, water spouts

1. INTRODUCTION

The dynamical processes occurring in our troposphere result in many remarkable signatures from the different physical process that modify the temperature and density structure, redistribute the species concentrations, and transport clouds and aerosols observed in the lower atmosphere. The dynamics in our lower atmosphere is so complicated because of the momentum provided by our rotating planet, combined with the orographic forcing of the atmosphere interface, the wide range of viscosity and roughness in interactions at the surface, and the daily oscillation of radiative heating, which force localized thermal convection. These processes are responsible for generating the planetary waves, weather fronts, gravity waves, low level jets, and turbulence eddies. The turbulence eddies result from thermal convection, and from wind shears at the surface, at the top of the boundary layer and tropopause layer, and throughout the troposphere wherever layers of wind shear occur. The most interesting signatures of the dynamical processes observed with Raman lidar are found in the water vapor and the aerosol profiles. In earlier papers, we have examined many processes that result in several of the unusual features that can be observed with lidar [1-11].

This paper examines the signatures of turbulent eddies and other related dynamical features in the lower troposphere. The features that we see in the Raman lidar profiles of water vapor are particularly interesting, because the cell structure observed in the water vapor appear to be the eddies expected in regions of turbulence. The water vapor profiles measured with Raman lidar provide the highest resolution signatures currently available for observing dynamical processes in the lower atmosphere. The lidar measurements of temperature and wind velocity would also be very interesting, but these techniques do not currently have sufficient space/time resolution to see the features that we observe in water vapor profiles. Standard rawinsonde balloons do exhibit small features in the vertical profiles but the measurement resolution in time and space is not sufficient to evaluate the turbulence structure. We have examined the interesting higher resolution measurements which can be obtained using tethered balloons with an instrument package that can be raised and lowered between the surface and about 300 m (limited by wind velocity and FAA rules).

*philbrick@ncsu.edu; phone 919-513-7174

Current models for understanding these measurements are based on Kolmogorov's early classical theory describing turbulence, which used the amplitude of fluctuations in the velocity of the atmospheric parcels as its basis. The idea is that larger scale dynamical processes provide the momentum and energy for the outer scale of turbulence and these large eddies, or turbules, beget smaller ones until the viscosity of the gas at the smallest scales dissipates the energy at the rate it is injected into the profile at the largest scale to form the eddy [see 12-16]. The eddies can be formed at large scales by several energy transfer processes: (1) localized thermal convection, (2) the rotational shear induced as wind moves atmospheric gases in contact with a surface, or goes around an object, (3) the velocity shear resulting from fast moving layers within the free troposphere, and when the faster moving free troposphere interacts with the top of the boundary layer, and (4) other types of dynamical process that can impart sufficient momentum into an air volume to form an eddy. The scale size of an eddy is determined by the interactions occurring during its initial formation, and is referred to as the outer scale of turbulence. Once an eddy is formed, its initial energy/momentum is transferred from this outer scale size to smaller scales within an eddy until it arrives at a sufficiently small scale that the ordered whirls of eddies become randomized at this inner scale of turbulence, and viscous dissipation of the energy occurs. The cascade of the momentum from the outer scale (10s or 100's of m to kms) to the inter scale (mm to cm) sizes are assumed to be non-dissipative, and is referred to as the inertial range of turbulence. The current views of turbulence consider the physical properties of the outer scale of turbulence eddies such as the temperature gradient and moisture gradient, which are recognized as being most important for optical propagation in describing index of refraction and the phase distortions of wave fronts at optical and RF wavelengths, when they encounter turbulence [16-21].

2. LIDAR DESCRIPTION

The Laser Atmospheric Profile Sounder (LAPS) is the fifth-generation Raman lidars that have been designed, fabricated, and used for research projects, since this work began in the late 1970's. This research effort was started four decades ago at the Air Force Cambridge Research Lab (AFCRL), moved to the Penn State University, in the Department of Electrical Engineering and the Applied Research Lab, in the late 1980s, and now resides in the NC State University Physics and MEAS Departments for the past seven years. Progress on the developments of commercial lasers, detectors, optical filters, and electronics have allowed these five generations of instrument advances. The LAPS instrument was designed to make simultaneous use of two of the four possible transmitter wavelengths of an Nd:YAG laser. Most of the experiments have been carried out using the 2nd and 4th harmonic wavelengths (532 nm and 266 nm, respectively) of an Nd:YAG high-power laser. The detector system for this instrument uses ten photon-counting PMTs, five for each wavelength, and each channel includes the dichroic beam-splitters and narrow-band filters needed to select vibrational and rotational Raman lines to be studied. The PMTs for the visible channels are only powered during the night to prevent overload damage to the individual detectors. The ultraviolet channels are used to collect data during all experiments since the signal wavelengths are in the solar-blind UV wavelengths. Even though the laser output power is much lower at the 4th harmonic, the signal-to-background advantage provides the most useful way to obtain 24-hr measurements. The primary Raman signals collected at both wavelengths usually include the first-Stokes vibrational scatter lines of N₂, O₂, and H₂O, and two groups of anti-Stokes rotational lines that are used for temperature profile measurements. One group of rotational lines is at lower J-levels near the peak intensity of the rotational Raman scatter, the second group is at higher J-levels, and both groups contain a combination of the N₂ and O₂ lines. The ratio of intensity of the high-J to low-J rotational lines of the molecules provides a direct measure of the atmospheric temperature. The scattered signal at the fundamental laser lines ($\Delta J = 0$) is often collected using a separate small telescope in a bistatic Rayleigh lidar mode to provide a measure of the backscatter ratio.

The N₂ vibrational Raman signal is used as a calibration reference for the measurements of water vapor. The profiles of major molecular signals (N₂, O₂, and the group of low-J rotational lines) are used for measurements of the aerosol optical extinction. The gradients in these profiles are compared with the hydrostatic profile calculated using the measured temperature profile, together with the surface measurements of temperature and pressure to determine the atmospheric density profile. A comparison of the differences in the slopes of the measured molecular profile to the hydrostatic profile, after accounting for the lidar two path length travel, is used to find the profile of optical extinction, at that wavelength. The optical extinction is the measure of the combined scattering and absorption that occurs between any two heights along the profile. The Raman lidar photon counting signals are integrated in bins of 75-meters in height and 1-minute in time. Profiles of water vapor are obtained from the ratio of signals of vibrational lines of H₂O to N₂, where the N₂ profile has been corrected for optical extinction by calculating the atmospheric density using the hydrostatic equation with the measured temperature profile, and accounting for the N₂ abundance. The profiles are stacked side by

side for each minute. The top of the profile is terminated when the error, based on SNR, becomes greater than $\pm 10\%$. A few times are blank at all altitudes when the lidar was shut down for maintenance or radar detection of a passing aircraft.

3. RESULTS

Raman lidar profiles of water vapor measured on the deck of the USNS Sumner in the Gulf of Mexico are shown in Fig. 1 to illustrate the signatures of turbulence and vorticity, when the specific humidity is used as a tracer of dynamical processes [22-26]. These results show dynamical features that are observed in the marine boundary layer, MBL, and the first 3 km of the free troposphere. Figure 1a profiles were obtained during sunset and nighttime in a period of relatively calm conditions, with only a few weak eddies during the early evening. Also observed are features below 100-m that would be interpreted as turbulence due to surface shear, if this were over land, but we disregard it here because it is probably due to the ship and its exhaust while underway in the Gulf. Near the end of this dataset an instability, identified by a low altitude SNR cut-off, is observed that is probably caused by buoyancy and a vorticity lifting moisture and forming small aerosols in the cooler air above the MBL can extinct the signal returns. This same action is observed several more times, in Fig. 1b during a transition from night into day, in Fig. 1c during daytime, and in Fig. 1d during the transition at sunrise. The two strong waterspouts observed in Fig. 1c exhibit rather impressive vortices. Several dozen such features were observed during approximately a month of cruising in the Gulf of Mexico and Atlantic along the Florida coast during September and October, over warm water. These features are observed rather frequently supplying moisture into the base of growing cumulus clouds, particularly when one considers that the instrument is only viewing vertically and only sees a very small cone of the atmosphere. They appear like double diffusive free convection, such as temperature and salt driven convection [15]. These instabilities are driven by a combination of temperature and water vapor mixing ratio (density). Another point is that Fig. 1d shows the development of strong plumes by thermal convection, and these occur at nighttime when the temperature of the atmosphere above the MBL is sufficiently cool to initiate thermal convection from the warm water surface.

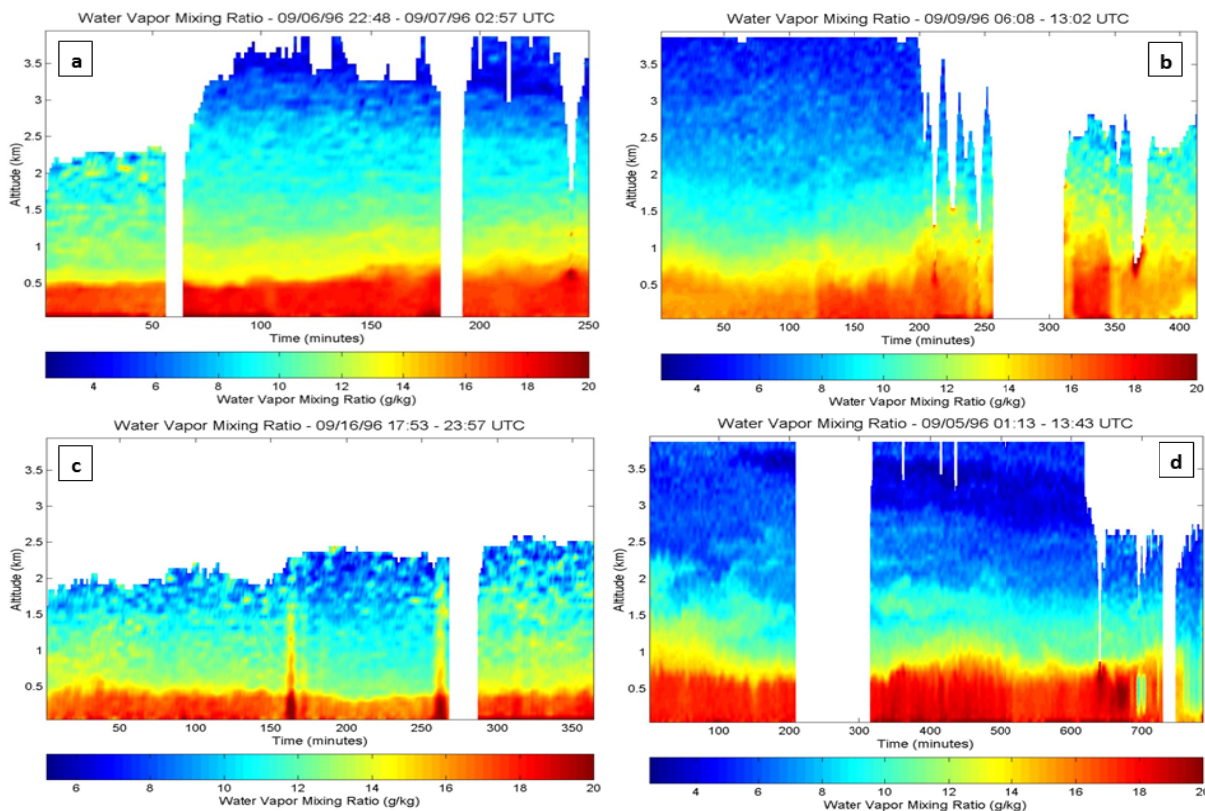


Figure 1. These four figures show a sequence of datasets with increases in the turbulent intensity. (a) Near laminar conditions are observed during the afternoon sunset and into the night (18:48-22:57 LT), but an instability occurs near end of this dataset (22:50 LT or 02:50 GMT) at the top of the MBL. (b) The atmosphere becomes very active at sunrise with water vapor being drawn upward into cloud formations above the MBL (02:08-09:02 LT). (c) Two striking water spouts are observed (12:53-19:57 LT). (d) Turbulence features occur at night (21:13-09:43 LT), and during sunrise as thermal convection draws additional water vapor to top of the MBL.

Figure 2 shows another set of lidar measurements on the USNS Sumner during nighttime and early morning, along with measurements from two rawinsonde balloon releases at the times indicated on the plot of the lidar data. The rawinsonde profiles of temperature, wind, and water vapor mixing ratio show the structure of the turbulence eddies, which we observe in the lidar data. Note the strong temperature gradient, which is the source of the water spout type of instabilities observed in Fig. 1. A comparison of the variation in the magnitudes of the profiles measured by the rawinsonde balloons further support the point made above, that the water vapor profiles provide the best signature for turbulent eddies due to their amplitude and ability to make sequential measurements. It is interesting that many of the features, such as changes in the gradients and inflections show up at the same altitude in the Temperature, Wind, and Mixing Ratio profiles.

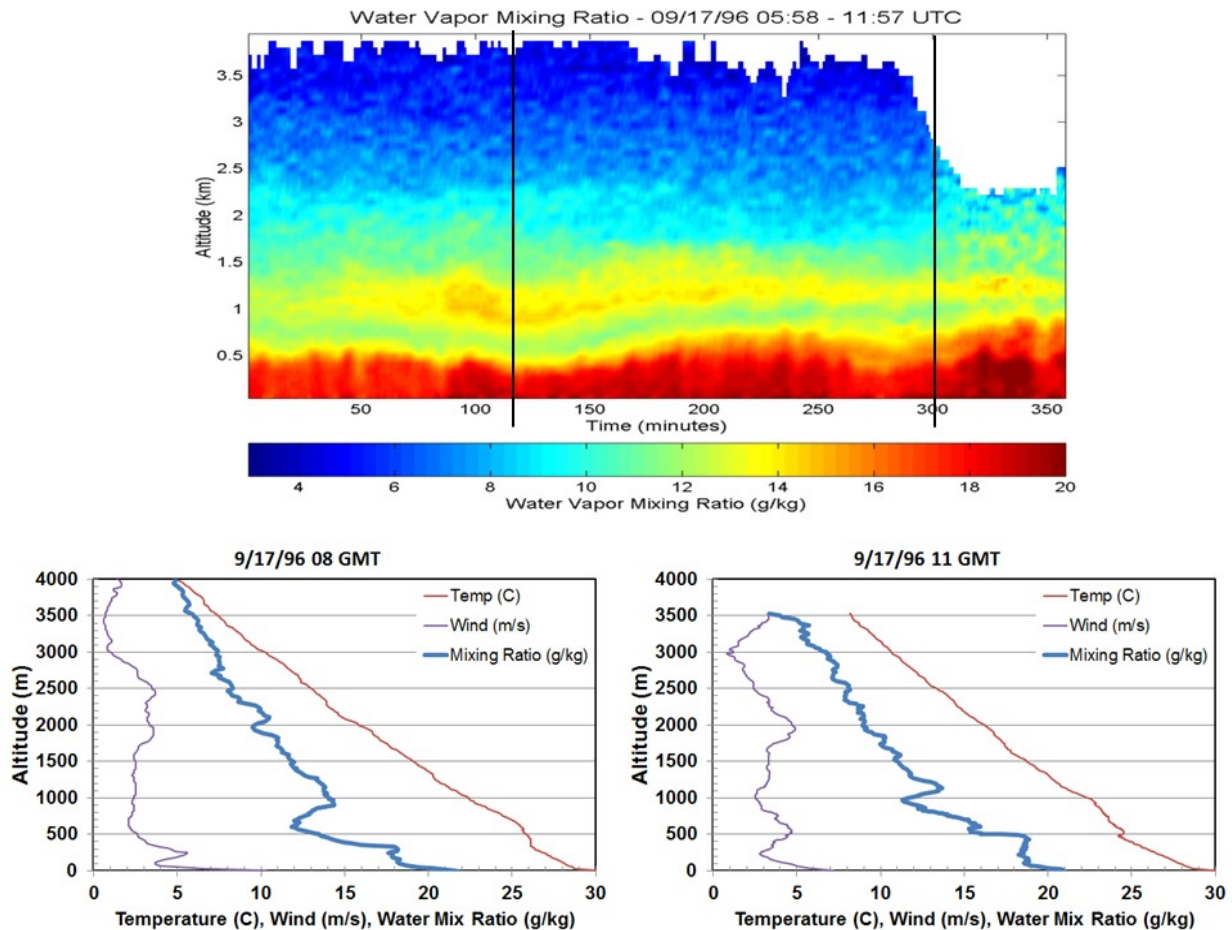


Figure 2. Profiles from lidar and rawinsonde balloons on the USNS Sumner are plotted for two times overlap (see location in the set of Raman lidar profiles) to show the relative magnitudes in variations of temperature, wind speed, and water vapor mixing ratio (disregard the bottom 200-m of the wind profiles from the moving ship).

The datasets in Fig. 1 and Fig. 2 demonstrate the importance of water vapor measurements in observing the dynamical processes in the marine atmosphere. This idea is also even more important for projects carried out over land surfaces, because surfaces contribute additional effects from localized areas of thermal convection and from forcing by orographic features and rough surfaces where wind shears generate turbulence. A sequence of one-minute vertical profiles obtained in a research program at a field site near Philadelphia during a 36-hr period is presented in Fig. 3. These measurements were conducted at a field site (NEOPS) located at the water treatment plant on the Hudson River near the Northeast Philadelphia Airport prepared in 1998, and this site was used for summer field measurements each year for seven years. Several laboratories collaborated on the field measurements to improve our knowledge of ozone as the effort under the North American Research Strategy for Tropospheric Ozone (NARSTO) Program. This particular two-day dataset is used to describe our approach for studying the turbulence processes in the lower atmosphere and results from several field programs have been published [1, 2, 6, 7, 9, 27-29].

The profiles shown in Fig. 3 include nighttime measurements which extend above the 3-km height of these plots when using the visible wavelengths at night, and daytime measurements using the solar-blind ultraviolet wavelengths only extend to about 2-km. The 1st panel in this figure shows that a moist layer is moving into the region. A calculation of the back-trajectory, using the NOAA air-mass trajectory model, shows that it came from the Ohio Valley and probably contains both the moisture and chemicals injected from the power plants located there. Between 6 AM and noon on this first day, the clear sky results in strong heating the surface and evaporation of the surface moisture to produce thermal convection plumes of turbulence that rise from 100-m to about 1400-m, and there intercept the air-mass arriving from the mid-west. The incoming air mass from the free troposphere is carrying water vapor and contains turbulent eddies, which appear to have a long lifetime, possibly due to shear of the moving air providing sufficient momentum to reenergize the eddies even as they are giving up energy by viscous dissipation at the small scale end of the inertial range. A major collision/interaction occurs between the transported air mass of the free troposphere and the freshly formed boundary layer about noon. This interaction appears to energize the turbulent eddies and fills them with more water vapor from the boundary layer. During the afternoon of 21 August, a major ozone and air pollution event occurred at our site, and an EPA mobile lab on site determined that the chemical, peroxyacyl nitrates (PAN), had caused the ozone and aerosol smog pollution event during the afternoon. At nighttime, the turbulent eddies, which have distributed themselves, probably with a bit of positive and negative buoyancy, before dissipating to distribute the moisture they carried in the nighttime boundary layer. These same datasets will be viewed in additional ways during the following discussion.

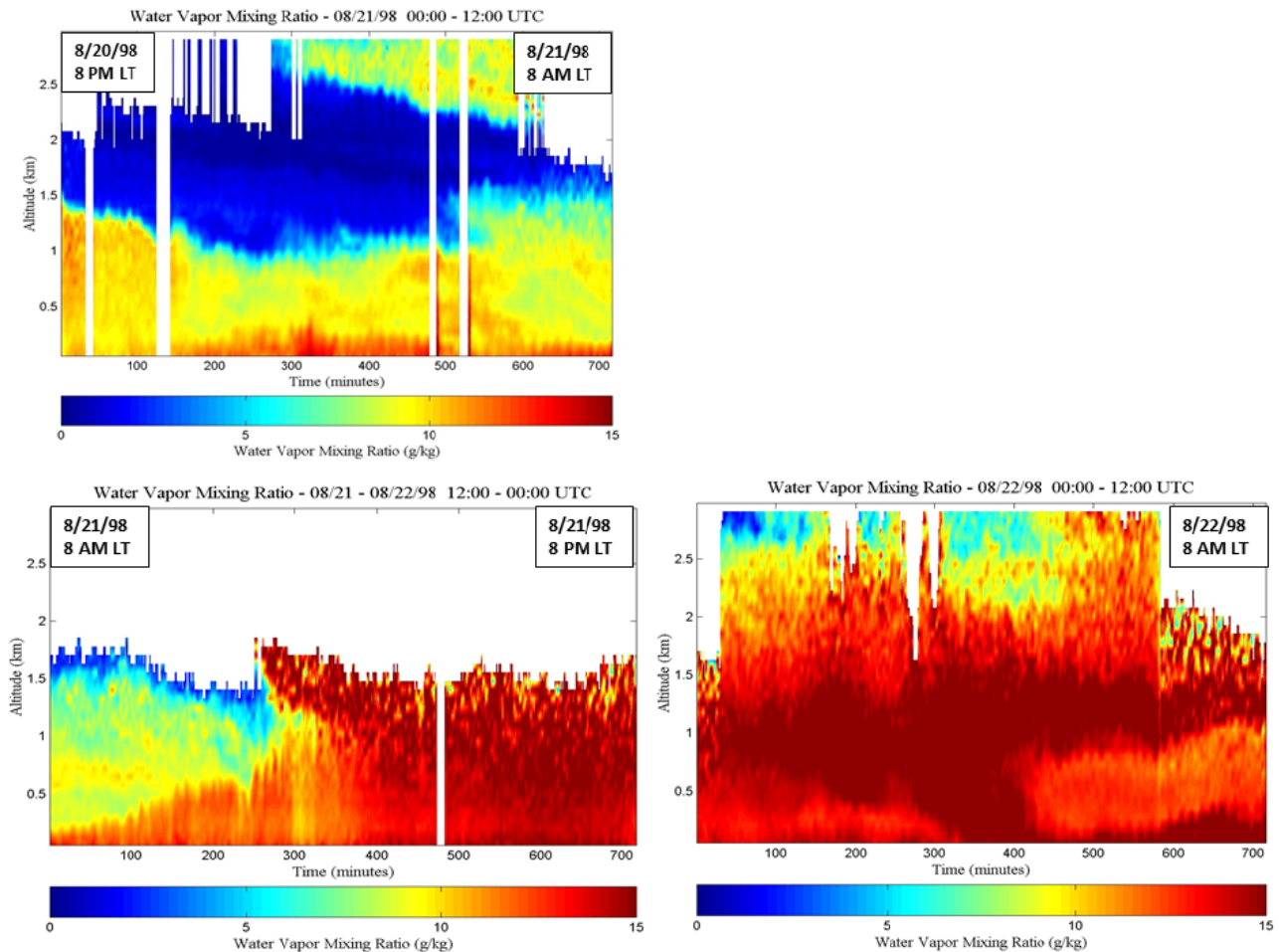


Figure 3. A 36-hr sequence of water vapor profiles show a transition from nighttime to the development of the daytime convective boundary layer, followed by the merging of an upper layer from the free troposphere with the rising morning boundary layer plumes near noon. The next day is an overcast day without the typical development of the daytime boundary layer.

In the 1st panel of Fig. 3, the moist layer entering the panel about midnight shows that it does contain turbulent eddies. The layer appears to have been traveling for some time and has characteristics of a faster moving layer, which has the capability to generate eddies and perhaps results in some entrainment by the action of shear at the layer boundary. Figure 4 shows a profile from the sum of 30 profiles at 3 AM LT. The SNR is increased sufficiently to observe the profile to 5-km altitude, and now the water vapor layer is observed to extend from ~2.5 to 4.0-km. About 4-hr after sunrise, the layer descends low enough to begin interacting with the boundary layer near 1.5-km as we see in the 2nd panel of Fig. 3. The interaction would cause shear induced turbulence eddies to form and possibly entrain water vapor from the boundary layer into decaying eddies carried in the jet. Once the cooler air from the higher altitudes interacts with the boundary layer to form turbules, their temperature will give them negative buoyancy. During the afternoon hours, eddies drift downward in the boundary layer and gradually dissipate, or at least become sufficiently small that they cannot be discerned with the current lidar resolution. It is expected that eddies will eventually dissipate, and they could distribute their water vapor as observed in the 3rd panel that shows the nighttime boundary layer.

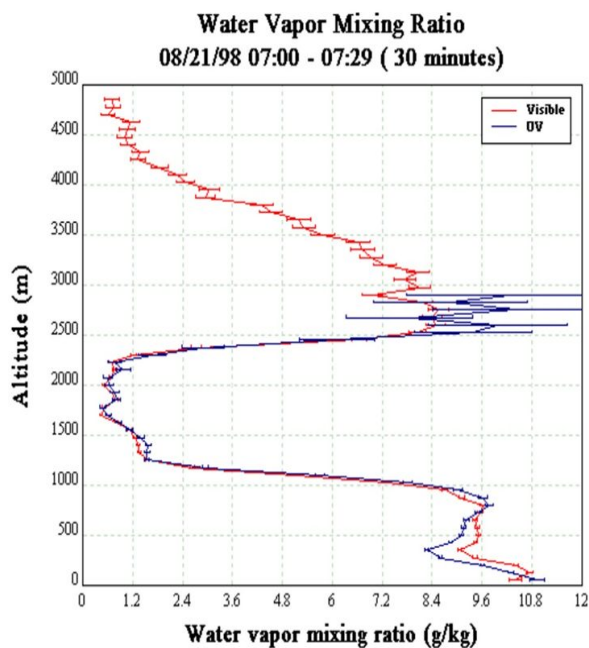


Figure 4. Adding 30 of the 1-minute files together, the water vapor profile is observed in the upper layer extending from 2.5 to 4-km at 03:00 LT.

The early analysis of turbulence considered the wind velocity as the starting point for developing its theory, but we have seen that temperature and water vapor also exhibit the characteristics of turbulent eddies. One additional set of data is now considered to answer the question: Is our present limit of our understanding of turbulence due to the observing tools that we use? The argument made here has been that the water vapor profiles measured by Raman lidar paint the optimum picture of turbulence, but was that just due to the poorer resolution of the wind and temperature measurements by a rawinsonde that was shown in Fig. 2. High resolution wind speed measurements were made by the research group of Prof. Richard Clark at Millersville University at the same time as the Raman lidar measurements. Figure 5 shows several of the data profiles they made using a cup anemometer and wind vane instrument that was raised and lowered by pulley to a large tethered balloon on a 30-min cycle. The slow ascent and descent resulted in high resolution measurements in both space and time. These wind measurements only cover the first 300-m, but since that allows measurements in the area where turbulent convection builds on clear morning, the data in Fig. 5 should hold the answer. And the answer is “yes” when the sequence of eight profiles measured in the tethered balloon are compared with the Raman lidar measurements of the turbulence near the surface. The first three profiles before sunrise show little variability in the profiles; however the next five profiles show a high variability in the wind profiles, which agrees well with the variations observations in the Raman lidar measurements. This demonstrates that careful measurements with high resolution sensors are needed to advance our understanding of turbulent eddies in the lower atmosphere.

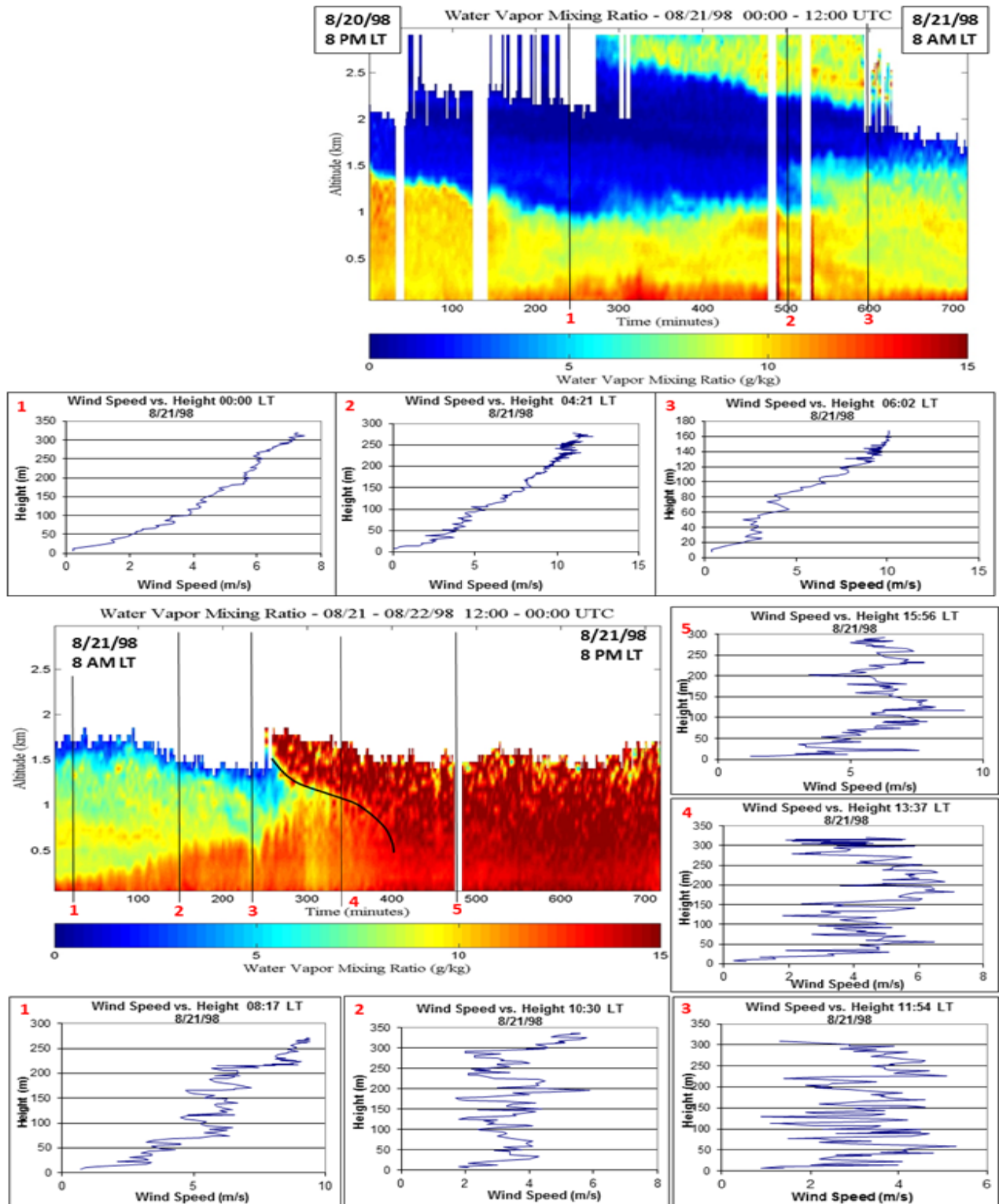


Figure 5. Two of the 12-hr time periods shown in Fig. 3 are used here marked to indicate when the Millersville University tether balloon instrument package made ascents to the balloon. A cup nanometer and a wind vane in the instrument package that was raised and lowered with a winch made high resolution measurements of the wind speed and direction from the surface to ~300 m.

Another question is interesting to consider: Are aerosols useful as tracers for the study turbulent eddies? That answer is probably, no, based upon the comparison of the aerosol optical extinction and the water vapor measured simultaneously by the Raman lidar. The measurements in Fig. 6 show an increase in extinction during the time after the turbulent eddies entered the boundary layer and added more water to their cells; however, at other times when we observe eddies, no aerosol signature is observed. Part of the problem is the aerosol growth and condensation, hence relative humidity strongly affects its relative importance, and it is difficult to distinguish such contributions from aerosol transport. This raises the question of a needed study regarding the condensation of very small aerosols and the scatter at the vibrational Raman wavelengths associated with them.

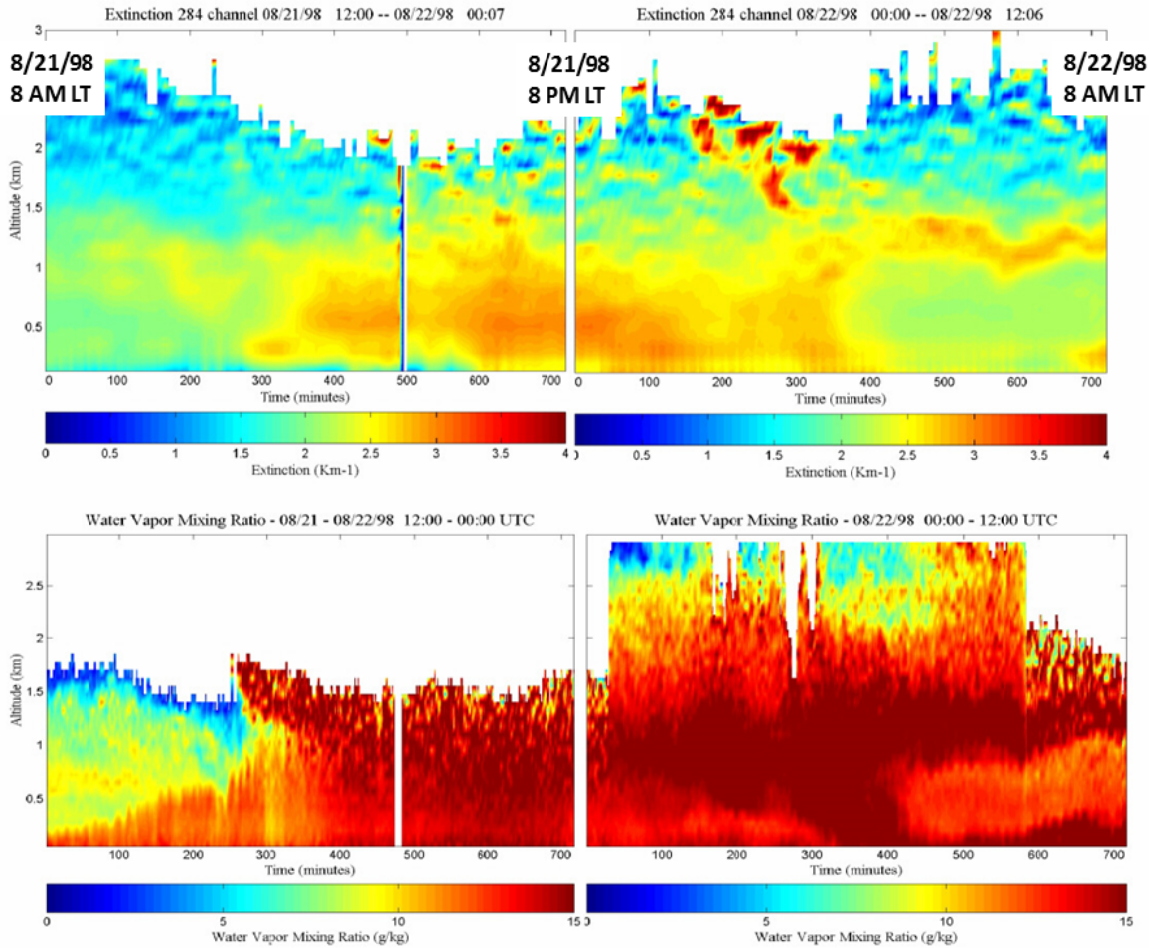


Figure 6. A 24-hr sequence of water vapor profiles is shown together with small particle aerosol extinction measured at 284 nm (N_2 vibrational Raman line) during the same period.

As examples of the rather wide range of signatures of dynamics observed in the water vapor profiles, four afternoon periods are shown in Fig. 7. These profiles of water vapor are from the Southern California Ozone Study conducted in 1997 [6, 27, 30]. The program included measurements at several locations and these are from a site at Hesperia CA in the high desert northeast of the Los Angeles basin. The regional dynamics and topography often causes the air mass in the valley to be lofted up into the desert above the location of the Raman lidar used in these experiments. These afternoon and evening periods show significant amounts of water vapor lofted out of the Los Angeles basin and into the atmosphere above the Mojave Desert. These water vapor profiles show a range of features of turbulence and the generation of waves and oscillations during transport of the air mass to our location.

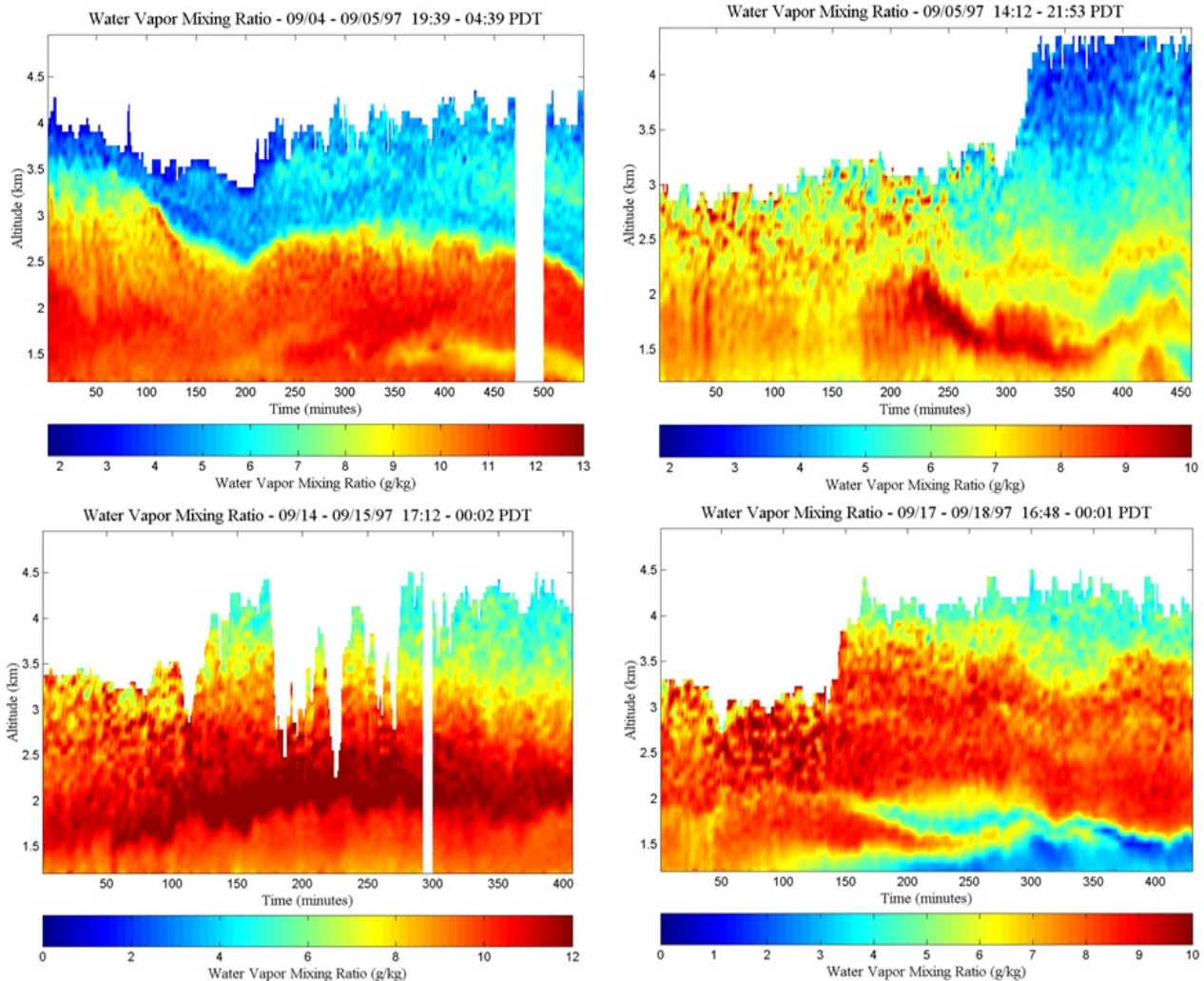


Figure 7. Four different sets of water vapor profile measurements during afternoon and nighttime conditions are selected to show the range of features observed during the Southern California Ozone Study (SCOS) project. These measurements were made at Hesperia CA (elevation 1200 m) where the regional conditions force unusual atmospheric features over the high Mojave Desert plateau at the north-eastern end of the Los Angeles basin.

SUMMARY AND PLANS

Examples of the measured signatures of dynamics by Raman lidar during three measurement campaigns (USNS Sumner, NEOPS, and SCOS) have shown the variety of dynamical processes active in the lower atmosphere. These examples point out the value in using high resolution profiles of water vapor as a tracer of the turbulence eddies present in the lower atmosphere. Many sets of data have been gathered by our research group over the past four decades, and they demonstrate that results from many campaigns contain interesting features which have not yet been fully analyzed, and reported, even though these measurements have been analyzed by more than 50 MS and PhD graduate students as part of their work degree work. While this research has been reported in their thesis, dissertations, and in more than 150 publications, the data was not analyzed in a consistent way, and it is not easy to assemble the data from multiple campaigns to examine many topics of interest. Our goal is to assemble the data from the campaigns into a common data base and prepare a more useful analysis program to provide opportunities for additional investigations using this data, and probably making the data base available to the research community. Based on our recent analysis, we also believe that a very useful direction for future research involves upgrading one of the earlier instruments with the currently available faster electronics, improved detectors, and better optical filter elements, to provide major improvements in the space and time resolution for future measurements.

ACKNOWLEDGEMENTS

The development of the current Raman lidar capability would not have been possible without the support of several funding agencies, particularly the DOD and DOE program managers, who have supported this research over the years. Many individuals have contributed much to the developments of the five generations of Raman lidar, particularly the graduate students involved in this research over the years. We thank Prof. Richard Clark for the use of his tethered balloon data and his meteorological insights in this study, and thank Prof. Pal Arya for his discussions and sharing his knowledge on the subject of turbulence. We also thank several colleagues, who were a great help in the early designs and development of the first two generations of Raman lidar, GLEAM and GLINT, in the 1970's and 80's: Dr. Dwight Sipler, Dr. Dan Lysak, and Byron Dix at AFCRL. After moving to Penn State University, the instrument work and dedicated research was the focused effort of outstanding PSU graduate students, with help from the Applied Research Laboratory and the ARL-PSU fabrication shops during the preparation of the LAMP, LARS, and LAPS lidars .

REFERENCES

- [1] Philbrick, C.R., Hallen, H.D., "Lidar investigations of atmospheric dynamics," Proc. SPIE, 9612, 96120C-1-16, (2015). doi: 10.1117/12.2188641
- [2] Philbrick, C.R., and Hallen, H.D., "Laser remote sensing of species concentrations and dynamical processes," Proc. SPIE 9080, 90800Z-1-15, (2014). doi: 10.1117/12.2050696
- [3] Balsiger, F., and Philbrick, C.R., "Comparison of lidar water vapor measurements using Raman scatter at 266 nm and 532 nm," Proc. SPIE 2833, 231-240, (1996).
- [4] Rajan, S., Kane, T.J., and Philbrick, C.R., "Multiple-wavelength Raman lidar measurements of atmospheric water vapor," Geophys. Res. Let. 21, 2499-2502, (1994).
- [5] Philbrick, C.R., "Raman lidar measurements of atmospheric properties," Proc. SPIE 2222, 922-931, (1994). doi: 10.1117/12.177985
- [6] Verghese, S.J., Willitsford, A.H., and Philbrick, C.R., "Raman lidar measurements of aerosol distribution and cloud properties," Proc. SPIE 5887, 100-107, (2005).
- [7] Wyant, A.M., Brown, D.M., Edwards, P.S., and Philbrick, C.R., "Multi-wavelength, multi-angular lidar for aerosol characterization," Proc. SPIE 7323, 73230R-1-8, (2009). doi: 10.1117/12.818686
- [8] Balsiger, F., Haris, P.A.T. and Philbrick, C.R., "Lower-tropospheric temperature measurements using a rotational Raman lidar," Proc. SPIE 2832, 53-60, (1996).
- [9] Novitsky, E. J., and Philbrick, C.R., "Multistatic Lidar Profiling of Urban Atmospheric Aerosols," J. Geophys. Res. Atmos. 110, D07S11, (2005).
- [10] Willitsford, A.H., and Philbrick, C.R., "Lidar Description of the Evaporative Duct in Ocean Environments," Proc. SPIE 5885, 140-147, (2005).
- [11] O'Brien, M. D., Stevens, T. D., and Philbrick, C. R., "Optical extinction from Raman lidar measurements," Proc. SPIE 2832, 45-52, (1996).
- [12] Arya, S. Pal, [Air Pollution Meteorology and Dispersion], Oxford University Press, New York, 310 pp. (1999)
- [13] Stull, R.B., [An Introduction to Boundary Layer Meteorology], Kluwer Academic Publishers, Boston, 666 pp. (1990).

- [14] Wyngaard, John C., [Turbulence in the atmosphere], Cambridge University Press, New York, 387 pp. (2010).
- [15] Tritton, D.J., [Physical Fluid Dynamics], 2nd edition, Clarendon Press, Oxford, 1988, p. 378-392 (1988).
- [16] Andrews, L.C., Phillips, R.L., [Laser beam propagation through random media], SPIE Press, Bellingham, 808 pp. (2005).
- [17] Mahrt, L., "Stratified atmospheric boundary layers," *Boundary-Layer Meteorol.* 90, 375-396, (1999).
doi:10.1023/A:1001765727956
- [18] Atlas, D., Metcalf, J.I., Richter, J.H., and Gossard, E.E., "The Birth of "CAT" and Microscale Turbulence," *J. Atmos. Sci.* 27, 903-913, (1970).
- [19] Kim, J., and Mahrt, L., "Simple Formulation of Turbulent Mixing in the Stable Free Atmosphere and Nocturnal Boundary Layer," *Tellus* 44A, 381-394, (1992).
- [20] Coulter, R.L., "A Case Study of Turbulence in the Stable Nocturnal Boundary Layer," *Boundary-Layer Meteorol.* 52, 75-92, (1990).
- [21] Moeng, Chin-Hoh, "A large-eddy-simulation model for the study of planetary boundary-layer turbulence," *J. Atmos. Sci.*, 41, 2052-2062, (1984).
- [22] Philbrick, C.R., Lysak, D.B., O'Brien, M., and Harrison, D.E., "Lidar Measurements of Atmospheric Properties," *Proc. Electromagnetic/Electro-Optics Performance Prediction Symposium*, Naval Post Graduate School, Monterey CA, 385-400, (1997).
- [23] Kiser, R.E., Davidson, K.L., and Philbrick, C.R., "The Generation and Characterization of Surf Zone Aerosols and Their Impact on Naval Electro-Optical Systems," *Proc. Electromagnetic/Electro-Optics Performance Prediction Symposium*, Naval Post Graduate School, Monterey CA, 355-375, (1997).
- [24] Philbrick, C.R., and Lysak, D.B., "Atmospheric Optical Extinction Measured by Lidar," *Proc. NATO-SET Panel Meeting on E-O Propagation*, NATO RTO-MP-1, 40-1 to 40-7, (1998).
- [25] Bas, C., and Philbrick, C.R., "Temporal and Spatial Characteristics of Surf Zone Plumes," *Proc. 20th Ann. Conf. on Atmos. Transmission Models*, 10-12 June 1997, AFRL-VS-HA-TR-98-0057 (AFRL Hanscom AFB, MA), 360-367, (1998).
- [26] Philbrick, C.R., "Raman Lidar Capability to Measure Tropospheric Properties," *Proc. 19th Int. Laser Radar Conf.*, NASA/CP-1998-207671/PT1, pp 289-292, (1998).
- [27] Philbrick, C.R., "Overview of Raman Lidar Techniques for Air Pollution Measurements," *Proc. SPIE*, 4484, 136-150, (2002).
- [28] Li, G., Chadha, G.S., Mulik, K.R., "Characterization of Properties of Airborne Particulate Matter from Optical Scattering Using Lidar," *Proc. PM2000:Particulate Matter and Health Conference AWMA*, W8-10, (2000).
- [29] Philbrick, C.R., Mulik, K.R., "Application of Raman Lidar to Air Quality Measurements," *Proc. SPIE*, 4035, 22-33, (2000).
- [30] Philbrick, C.R., "Raman Lidar Characterization of the Meteorological, Electromagnetic and Electro-optical Environment," *Proc. SPIE*, 5887, 85-99, (2005).